Hindawi
Journal of Nanomaterials
Volume 2022, Article ID 1832587, 11 pages
https://doi.org/10.1155/2022/1832587

Research Article

Green Synthesis of Silver Nanoparticles from Root Extracts of *Rubus ellipticus* Sm. and Comparison of Antioxidant and Antibacterial Activity

Lekha Nath Khanal,[1,2] **Khaga Raj Sharma**,[1] **Hari Paudyal**,[1] **Kshama Parajuli**,[1] **Bipeen Dahal**,[1] **G. C. Ganga**,[3] **Yuba Raj Pokharel**,[4] **and Surya Kant Kalauni**[1]

[1]*Central Department of Chemistry, Tribhuvan University, Kathmandu, Nepal*
[2]*Department of Chemistry, Prithvi Narayan Campus, Tribhuvan University, Pokhara, Nepal*
[3]*Central Department of Microbiology, Tribhuvan University, Kathmandu, Nepal*
[4]*Faculty of Life Science and Biotechnology, South Asian University, New Delhi, India*

Correspondence should be addressed to Surya Kant Kalauni; skkalauni@gmail.com

Received 12 January 2022; Revised 23 February 2022; Accepted 1 March 2022; Published 11 March 2022

Academic Editor: Thathan Premkumar

Copyright © 2022 Lekha Nath Khanal et al. This is an open access article distributed under the Creative Commons Attribution License, which permits unrestricted use, distribution, and reproduction in any medium, provided the original work is properly cited.

The fabrication of metal nanoparticles through green synthetic pathways using plant extracts has increased attention due to low cost, benevolent methods, fewer hazardous byproducts, and applications. Silver nanoparticles (AgNPs) were synthesized by reacting to aqueous root extracts of *Rubus ellipticus* Sm. (RERE) with $AgNO_3$ solution (1 mM) at an ambient condition. The visual change of color from light yellow to reddish brown and the absorption peak at 416-420 nm in the UV-visible spectra indicated the formation of AgNPs in the solution. The shifting of the positions in the FTIR spectra indicated the potential role of the functional groups as capping and stabilizing agents. The powder XRD diffractogram exposed the crystalline nature of the nanoparticles. The surface morphology and the elemental composition of the AgNPs were established by the FESEM and EDX analysis. The TEM images revealed the spherical and monodispersed nanoparticles of size ranging from 13.85 to 34.30 nm with an average of 25.20 ± 7.01 nm ($n = 10$). The biogenic AgNPs showed a better 2,2-diphenyl-1-picrylhydrazyl (DPPH) radical scavenging activity with lower IC_{50} ($13.83 \pm 0.33\ \mu g/mL$) as compared to that of the RERE with IC_{50} ($15.86 \pm 4.14\ \mu g/mL$). The synthesized AgNPs showed higher zones of inhibition (ZOI) on the agar well diffusion method against *Enterococcus faecalis* (ATCC 29212), *Escherichia coli* (ATCC 25922), *Staphylococcus aureus* (ATCC 25923), and *Klebsiella pneumoniae* (ATCC 700603). The result of this study highlights the potential benefits of *R. ellipticus* root extract-based AgNPs for biomedical practices.

1. Introduction

Nanotechnology is emerging as an extensive interdisciplinary area of research all over the world for a few decades. The design, manufacturing, characterization, and application of nanoparticles have increased attention due to their unique physical and chemical properties [1]. Generally, nanoparticles are extremely small particles with their size ranging from 1 to 100 nm and exhibit completely new properties compared to that of bulk materials. They have a higher surface area to volume ratio, which brings the variation in the other specific parameters like size, distribution, and morphology. The higher surface area of the AgNPs is responsible for their increased catalytic and biological properties [2]. The nanoparticles of noble metals like gold, silver, palladium, and platinum are extensively used in various industrial and pharmaceutical practices due to their incredible physicochemical, optical, and biological properties [3].

Silver is a safe antibacterial metal that is reported to kill more than 650 pathogenic bacteria, and many researchers are involved in the synthesis of silver nanoparticles (AgNPs) because of their higher antimicrobial nature

[4]. Nowadays, silver nanoparticles are used in diverse fields such as electronics, optics, photography, clothing, catalysis, dentistry, and food industries. Besides, it has immense application in biomedical fields such as biomolecular detection, biosensors, and antifungal, antibacterial, and antiangiogenetic agents [5, 6].

Conventionally, AgNPs are synthesized by various physical methods, e.g., evaporation-condensation, arc discharge, and spray pyrolysis, and chemical methods, e.g., photochemical and electrochemical reduction, Tollens's method, and sonochemical methods. These approaches suffer from the complications like the use of expensive and hazardous chemicals as well as the formation of toxic byproducts [7, 8]. The investigates are focused on the "green synthesis" methods as a substitute for orthodox procedures by using biological extracts such as plants, fungi, algae, and microbes [1]. The extract of a brown algae *Sargassum longifolium* was used for the synthesis of AgNPs which significantly inhibited the growth of pathogenic fungi *Aspergillus fumigatus*, *Candida albicans*, and *Fusarium* species by the agar well diffusion method [9]. *The mycogenic Penicillium chrysogenum*-derived AgNPs having an average size of 48.2 nm inhibited the process of biofilm formation by 90% against *Acinetobacter baumannii* (ATCC 19606) at the concentration of 2 μg/mL [10]. The AgNPs biosynthesized from the cultures of *Candida albicans* and 1.5 mM $AgNO_3$ with the size range of 20-80 nm exhibited significant antibacterial activity against *Escherichia coli* and *Staphylococcus aureus* [11]. The biogenic AgNPs synthesized having an average size of 15 nm from the cultures of *Corynebacterium glutamicum* were reported to exhibit enhanced antibacterial activity against *Escherichia coli*, *Shigella flexneri*, *Salmonella enterica*, *Klebsiella pneumoniae*, *Staphylococcus aureus*, *Pseudomonas aeruginosa*, *Bacillus flexus*, and *Bacillus subtilis* by the agar well diffusion method [12]. The commercial production of nanoparticles using microbes is less manageable as it needs highly aseptic conditions and proper maintenance. The use of plants for this purpose is more advantageous due to lesser biohazards and benign methods as well as no risk of chemical contamination [5, 13]. In comparison to other green methods, plant-based approaches are easy, quick, safe and result in the formation of stable nanoparticles having fewer side effects [14]. Diverse secondary metabolites in plants like flavonoids, terpenoids, ketones, carboxylic acids, amides, proteins, and enzymes act as reducing, capping, and stabilizing agents and therefore facilitate the bioreduction and precipitation of AgNPs, which are safe and cost-effective [15–17]. The increase in antimicrobial effectiveness of green synthesized AgNPs is due to the presence of antimicrobial materials in the extract. The contemporary literature comprises many reports of synthesis, characterization, and applications of plant-mediated AgNPs. The green synthesized AgNPs from the leaf extract of *Pongamia pinnata* were reported to exhibit substantial antioxidant activity [18]. The biosynthesized AgNPs from the leaf extract of *Chenopodium murale* with sizes ranging from 30 to 50 nm exhibited elevated antioxidant and antimicrobial activities [19]. A medicinal plant, *Eriobotrya japonica*, collected from Iraq was used for the green synthesis of AgNPs. The crystalline nanoparticles having a size ranging from 17 to 35 nm were reported to inhibit the cancer cell proliferation and induced apoptosis. They decreased the IL-beta and IL-6 levels *in vivo* as well as *in vitro* models [20]. Similarly, biogenic AgNPs synthesized from the fruit extract of *Emblica officinalis*, leaves of *Citrus limon*, *Camellia sinensis* (green tea), *Coffea arabica* (coffee), etc. were characterized by proper procedures and accessed for their biological activities [13]. Moreover, the green synthesized AgNPs from the stem and root extracts of *Lysiloma acapulcensis* exhibited higher antimicrobial activity than chemically synthesized AgNPs. The values of the zone of inhibition (ZOI), minimum inhibitory concentration (MIC), and minimum bactericidal concentration (MBC) against *Escherichia coli*, *Pseudomonas aeruginosa*, *Staphylococcus aureus*, and *Candida albicans* of green AgNPs are higher than those of chemically synthesized AgNPs [21].

Rubus ellipticus Sm. (Rosaceae) is abundant in the wide areas of forest edges in the elevations of 548-1700 m in various parts of Asia and other continents. Different parts of the plant are reported to show various biological activities such as antidiabetic, antioxidant, antimicrobial, wound healing, and antitumor [22, 23]. It is also known as Himalayan raspberry and is locally named "Yensalu." The methanol root extract of the plant exhibited significant antioxidant and antimicrobial properties [24]. The synthesis and characterization of AgNPs from *R. ellipticus*roots have not been reported to our information. Therefore, this study is aimed at synthesizing and comparing the antioxidant and antimicrobial activities of the biogenic AgNPs with that of aqueous extract of *R. ellipticus.*

In this research, a new and green route is explored for the synthesis of AgNPs in which the phytochemicals present in the root extract of *R. ellipticus* reduced Ag^+ ion into elemental AgNPs. The UV-visible and Fourier-transform infrared (FTIR) spectroscopy, scanning electron microscopy (SEM), transmission electron microscopy (TEM), and powdered X-ray diffraction (XRD) methods were used for the characterization of the AgNPs. The synthesized AgNPs were analyzed for the comparative antioxidant and antibacterial activities.

2. Materials and Methods

2.1. Materials and Reagents. The root barks of the plant were collected from the outskirts of Pokhara city in the Gandaki province of Nepal in July 2020. The proof of identity of the plant was taken from the National Herbarium and Plant Laboratories, Godawari, Nepal. The root barks were cleaned and rinsed with distilled water properly. The barks were shade-dried for four weeks and converted into a fine powder using a mechanical mill. Analytical grade reagents and deionized water were used throughout the experiment. Silver nitrate, dimethyl sulphoxide, and methanol were purchased from Thermo Fisher Scientific India Pvt. Ltd.; neomycin, Muller Hinton Agar (MHA), and Muller Hinton Broth (MHB) of Himedia Pvt. Ltd. India and DPPH of Tokyo Chemical Industries Co. Ltd. Japan were used.

2.2. Preparation of Plant Extract. Five grams of root powder was added to 50 mL of distilled water in an Erlenmeyer's flask of 250 mL capacity. The mixture was heated carefully for about 15-20 minutes and was filtered through a Whatman filter paper (no. 1). The prepared aqueous extract was stored at 4°C and used within a week.

2.3. Biosynthesis of Silver Nanoparticles. 5 mL of the fresh RERE was dropped into 45 mL of $AgNO_3$ (1 mM) solution with constant stirring on a magnetic stirrer at 25 ± 2°C [25–27]. The light yellow color of the solution started to change gradually and turned reddish brown within one hour. It was considered as a visual sign of the growth of AgNPs. After the completion of the reaction, the solution was centrifuged at 8000 rpm for 40 minutes at 20°C and repeatedly washed three times. It was collected and further centrifuged at 14000 rpm with double-distilled water for 20 minutes. Finally, it was dehydrated by ethanol, dried using a desiccator, and stored for the necessary characterization and biological studies.

2.4. Characterization of AgNPs

2.4.1. UV-Visible and FTIR Spectroscopy. The absorption spectra of synthesized AgNPs were recorded by using UV-visible spectroscopy from 300 to 600 nm (BioTek, Synergy LX multimode reader) at the intervals of 15 minutes, 50 minutes, 18 hours, and 48 hours by taking distilled water as blank. The FTIR spectra of the solid RERE and AgNPs were taken by a Shimadzu IRTracer-100 from 4000 to 400 cm^{-1}. It helped to detect the functional groups in the extract and the AgNPs that might be accountable for synthesizing the nanoparticles.

2.4.2. X-Ray Diffraction (XRD) Analysis. An X-ray diffractometer (Rigaku Co., Japan) was used to confirm the crystallinity of the synthesized AgNPs. The diffractogram was obtained from the dried layer of the sample over a sample holder by using CuKα ($\lambda = 1.5406$ Å) radiation with 30 mA of current and 40 kV of voltage in a scan rate of 10°/minute across the 2θ angle ranging from 0 to 90 [20].

2.4.3. FESEM, EDX, and TEM Analysis. The suspension of AgNPs was spread uniformly and dehydrated over a cover glass and placed on a copper stub attached with carbon tape. The TEM images and selected area electron diffraction (SAED) pattern were taken by using a JEM-2100 plus at 200 kV (JEOL Ltd., Japan). The images were taken by coating the suspension of AgNPs over a carbon-coated copper grid. The size of the synthesized AgNPs was measured with the help of ImageJ software from the TEM images.

2.5. In Vitro Antioxidant Activity. The DPPH free radical method was used to assess the antioxidant activity of the RERE and the AgNPs with minor adjustments [28, 29]. Briefly, the solutions of 500, 250, 125, 62.5, 31.25, and 15.62 μg/mL were prepared by serial dilution in 50% dimethyl sulphoxide (DMSO). Aliquots of 100 : 100 μL of the test solutions and DPPH (0.1 mM) were filled in the bores of a 96-well microplate with negative and positive controls in triplicates. Then, the microplate was put in the dark at room temperature for 30 minutes. The absorbance of the solutions was recorded by using a microplate reader at 517 nm. The percentage scavenging (%Sc) of the samples was calculated by applying

$$\%\mathrm{Sc} = \frac{A_b - A_t}{A_b} \times 100, \quad (1)$$

where A_b and A_t are the absorbances of the blank and test sample, respectively. The DPPH free radical inhibition activity of the RERE and the synthesized AgNPs at different concentrations was plotted and compared with that of ascorbic acid. The concentration corresponding to 50% inhibition (IC_{50}) was calculated.

2.6. Antimicrobial Activity

2.6.1. Microorganisms. The antibacterial tests were made by taking the pure cultures of bacteria from the American Type Culture Collection (ATCC). They were subcultured and stored into the Muller Hinton Agar (MHA) media at 4°C. The organisms used in the test are listed in Table 1.

2.6.2. Agar Well Diffusion Assay. The agar well diffusion method was adopted to observe the antibacterial susceptibility [30]. The test bacteria were grown in the Muller Hinton Broth (MHB) so that the turbidity equals that of 0.5 McFarland's standard (1.5×10^8 CFU/mL). Aliquots of 30 μL of the RERE, synthesized AgNPs, negative and positive controls were loaded into the wells of 6 mm diameter and incubated for 24 hours at 37°C. On the next day, the plates were taken out from the incubator, and the clear regions formed around the wells were recorded as the corresponding zones of inhibition (ZOI).

2.6.3. Statistical Analysis. The experiments were performed in triplicates, and the results were presented as mean ± standard deviation. The raw data of antioxidant activities were processed by using Gen5 Microplate Data Collection and Analysis Software and then by Microsoft Excel. The FTIR data of AgNPs and the plant extract were plotted in "Origin 19b." The concentration corresponding to 50% inhibition (IC_{50}) was determined with the help of GraphPad Prism 9 software.

3. Results and Discussion

3.1. UV-Visible and FTIR Spectroscopy. Various methods have been used for the synthesis of metallic nanoparticles. The biosynthetic method is safe and ecofriendly and uses secondary metabolites in the plant extract for the reduction. The addition of RERE to 1 mM of silver nitrate solution with constant stirring led to the change of color of the solution from yellowish to reddish brown. It is due to the excitation of surface plasmon resonance (SPR) variations in the biosynthesized nanoparticles [31].

The synthesis of AgNPs was monitored at different time intervals by the change of color and absorption spectra appeared at around 416-420 nm by UV-visible spectroscopy

Table 1: List of bacteria used for the test.

Bacteria	Type	ATCC
Escherichia coli	Gram-negative	25922
Enterococcus faecalis	Gram-positive	29212
Staphylococcus aureus	Gram-positive	25923
Klebsiella pneumoniae	Gram-negative	700603

as shown in Figure 1. The biosynthesized silver nanoparticles of *Rheum australe* extract of Indian origin showed solid absorption bands between 410 and 420 nm indicating the presence of polydispersed particles which agrees with our result [32]. Change of color from golden yellow to pinkish brown was observed in the reduction of Ag^{+} to Ag° in the colloidal solution. A sharp absorption peak at 420 nm was observed in the UV-visible spectroscopy during the biosynthesis of AgNPs from the *Tagetes erecta* aqueous leaf extracts [33]. The strong broad absorption band obtained between 405 and 430 nm for silver nanoparticles indicates that the spherical particles were dispersed without aggregation [34, 35]. Venkatesan et al. [36] reported the SPR peak of the biosynthesized silver nanoparticles at 418 nm upon 18 hours of formation by UV-visible spectroscopy. They prepared the AgNPs from the aqueous extract of marine algae *Ecklonia cava* and the intensity of the peak increased with time which is analogous to our results. The positions of the peaks in the FTIR spectra of RERE and the AgNPs were compared to check the functional groups involved in the capping and stabilizing actions. The IR spectra of RERE and the AgNPs were recorded for different functional groups in the range of 400–4000 cm^{-1} shown in Figure 2. In the spectra, a broad peak at 3240.31 cm^{-1} in the extract is shifted to 3302.76 cm^{-1} in the AgNPs. It is due to the stretching frequency of a hydrogen-bonded -OH group of polyphenols present in the plant [15].

Similarly, the shifting of vibrations at 1039.63 to 1029.98 cm^{-1} corresponds to the C-O stretching of ether linkages present in the flavones which are adsorbed on the surface of the biogenic AgNPs [17, 37]. The peak at 2927.27 cm^{-1} in the RERE is moved to a higher wavenumber of 2939.92 cm^{-1} in the AgNPs corresponding to the stretching of SP^3-hybridized C-H of alkanes or aldehydes [38]. The FTIR peaks which are observed at 1724.90 cm^{-1} and 1600.00 cm^{-1} correspond to the presence of C=O and C=C or aromatic C=C bonds. The change of the position of the peaks of RERE from 1312.25 to 1321.23 cm^{-1} AgNPs corresponds to the stretching of a carbon-nitrogen bond of aromatic amines. The peaks of vibrations at 1174.64 cm^{-1} are observed.The shifting of the peaks of O-H or N-H stretching and double and triple bonds of hydrocarbons in the FTIR spectra were observed in the green synthesis of AgNPs [37, 39].

3.2. X-Ray Diffraction Analysis. Based on Bragg's reflections for a face-centered cubic (fcc) structure of silver, the diffractogram indicated the AgNPs to have a crystalline geometry. The nature of the XRD plot of our AgNPs was matched to the pattern of JCPDS (Joint Committee on Powder Diffraction Standards) file number 03-0921 (Figure 3). There are four intense peaks at the 2θ angles of 37.87, 44.02, 64.24, and 77.24 corresponding to the hkl values of 111, 200, 220, and 311 planes matching to the fcc crystal. This structure of our AgNPs is parallel to the XRD pattern of the synthesized silver nanoparticles from aqueous extracts of *Lysiloma acapulcensis* [21]. The relative position of peaks at the 2θ angles in the XRD pattern of the biosynthesized AgNPs of ethanol extracts of Indian Sandalwood (*Solanum album*) is like to our result indicating the formation of nanoparticles having equivalent geometry [40]. The organic molecules in the RERE that are tangled in the reduction and stabilization of AgNPs are responsible for the peaks in the XRD analysis [26].

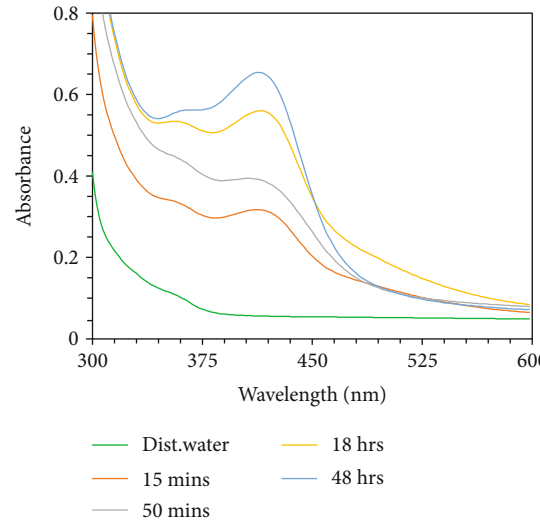


Figure 1: UV-visible spectra of AgNPs at different times.

3.3. FESEM, TEM, and EDX Analysis. The surface morphology of the nanoparticles was observed by scanning electron microscopy with different resolutions. The FESEM images show the particles like broken lumps at the low resolution of 15.2 mm × 100 to clear agglomerates of spherical, oval, or bead-like units of the nearly same size at a higher magnification of 9.2 mm × 150 k as shown in Figures 4(a)–4(d). The single SPR peak observed in the UV-visible spectra of biosynthesized AgNPs suggests the formation of spherical particles which is further confirmed by SEM micrograph [25]. The qualitative and quantitative status of the component elements in AgNPs was recognized by the EDX spectrum. Figures 5(a) and 5(b) show the elemental mapping of synthesized AgNPs that demonstrates the existence of silver, carbon, oxygen, chlorine, and calcium. The existence of an intense peak at 3 keV of Ag° with the highest counts confirms the formation of silver particles [41].

The EDX result shows different peaks of oxygen (0.52 keV), carbon (0.28 keV), calcium (3.69 and 4.12 keV), and chlorine (2.62 keV) in trace amounts (Figure 5(b)). These peaks might be attributed to the contamination of organic materials and carbon tape used in the measurement process. The TEM images (Figure 6) were observed to find the shape and size of the synthesized AgNPs. Most of the nanoparticles are spherical; some are irregular and dispersed

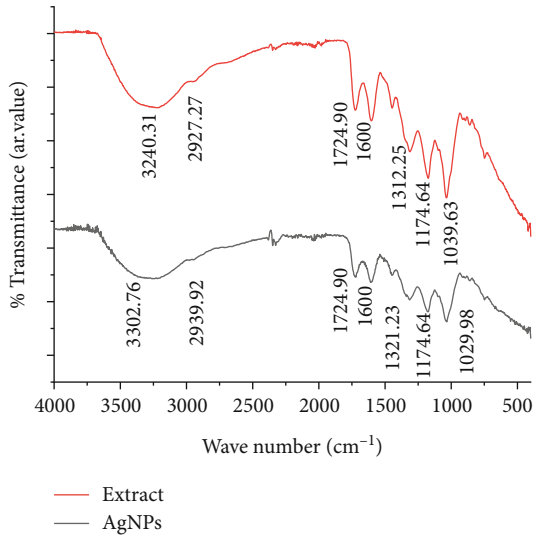


Figure 2: Comparative study of FTIR spectra of RERE and AgNPs.

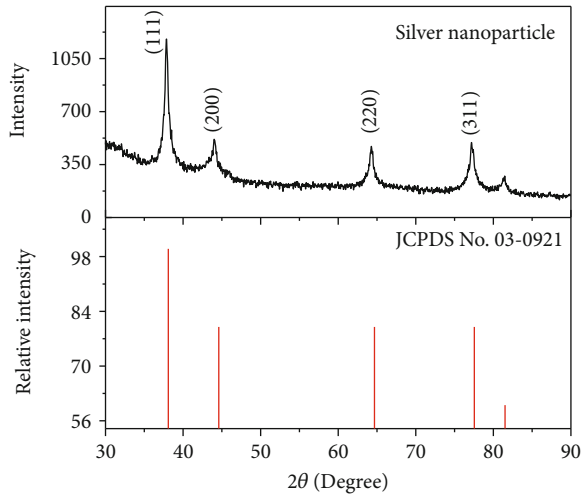


Figure 3: X-ray diffraction (XRD) patterns of synthesized AgNPs and JCPDS no. 03-0921.

with minor agglomeration (Figure 6(a)). The nanoparticles had a size variation from 13.85 to 34.30 nm with an average of 25.20 ± 7.01 nm ($n = 10$) which is shown in the histogram (Figure 6(b)).

The spherical shape and coarse exterior are seen in the TEM image of a single typical AgNPs which have a diameter of 23 nm (Figure 6(d)). There are four diffraction rings equivalent to the fcc planes of (1 1 1), (2 0 0), (2 2 0), and (3 1 1) in the selected area electron diffraction (SAED) diagram of the biogenic AgNPs (Figure 6(c)). Comparable to our observation, the TEM images of the plant-mediated AgNPs prepared by using aqueous leaf extract of *Artocarpus altilis* were also reported an fcc structure and size extending from 20 to 50 nm [42]. Suman et al. [43] reported the size of AgNPs ranging from 32 to 55 nm synthesized by using the root extracts of *Morinda citrifolia* collected from Mangalore, India, is comparable to our result.

3.4. In Vitro Antioxidant Activity. The results of *in vitro* radical inhibiting potential of the AgNPs and RERE against DPPH are presented in Table 2. We observed that the biosynthesized AgNPs were found to be more potent antioxidants than the aqueous root extract of *Rubus ellipticus*. Figure 7 illustrates that the synthesized AgNPs had a higher percentage inhibition in comparison to that of the crude extract at different concentrations. The AgNPs were found to be more powerful antioxidant ($IC_{50} = 13.83 \pm 0.33\,\mu g/mL$), than the RERE ($IC_{50} = 15.86 \pm 4.14\,\mu g/mL$). Ascorbic acid taken as positive control exhibited the highest activity ($IC_{50} = 6.40 \pm 0.29\,\mu g/mL$) as shown in Table 3. A separate study reported that biochemically synthesized AgNPs at an ambient temperature had relatively higher antioxidant activity over aqueous extract of the rhizome of *Rheum australe* collected from Jammu and Kashmir, India [32].

The radical scavenging activity of the synthesized AgNPs was higher than that of *Prosopis farcta* aqueous fruit extract at different concentrations. The higher activity of the biogenic nanoparticles was described due to the abundance of phenolic and flavonoid contents in the extract in comparison to the AgNPs [6]. The AgNPs synthesized using aqueous leaf extracts of *Costus afer* collected from Nigeria also showed higher radical scavenging activity. The advanced activity of the synthesized AgNPs is explained due to the simultaneous mechanisms of hydrogen atom transfer (HAT) and single electron transfer (SET) of flavonoids and silver ions present in the AgNPs [44]. Similarly, the DPPH radical scavenging capacities of AgNPs were increased in comparison to the corresponding extracts which are analogous to our results [36, 45]. The AgNPs synthesized from the rhizome extract of *Bergenia ciliata* of Pakistani origin exhibited an elevated DPPH radical scavenging activity and cytotoxicity against Brine shrimp nauplii ($LD_{50} = 33.92\,\mu g/mL$) than the crude extracts [46].

The secondary metabolites such as phenolics, flavonoids, terpenoids, and soluble proteins act as capping agents for the synthesis of nanoparticles [47]. The electron-donating potential of polyphenols in the plant extracts facilitated the bioreduction of Ag^{+} to Ag° and stabilized the AgNPs. Similarly, the water-soluble flavonoids in plants are also involved in the reduction of silver ions for the synthesis of AgNPs [38]. Important phytochemicals like flavonoids, polyphenols, saponins, terpenoids, and vitamins are responsible for the antioxidant activity of the plant extracts. We have also reported the abundance of these phytochemicals in the roots of *R. ellipticus* collected from the same site [24]. The compounds may have adsorbed on the larger surface area of the spherical AgNPs and amplified the antioxidant potential. The negatively charged phytochemicals exhibit an electrostatic attraction to the positively charged or neutral AgNPs which also synergically improved the bioactivity [48].

3.5. Antibacterial Activity. Most of the AgNPs exhibit significant antimicrobial actions against various bacteria, fungi, and viruses. So, they have been extensively used in many common products like bandages, plasters, catheters, blades, cosmetics, toothbrushes, and cellphones [49]. Here, both

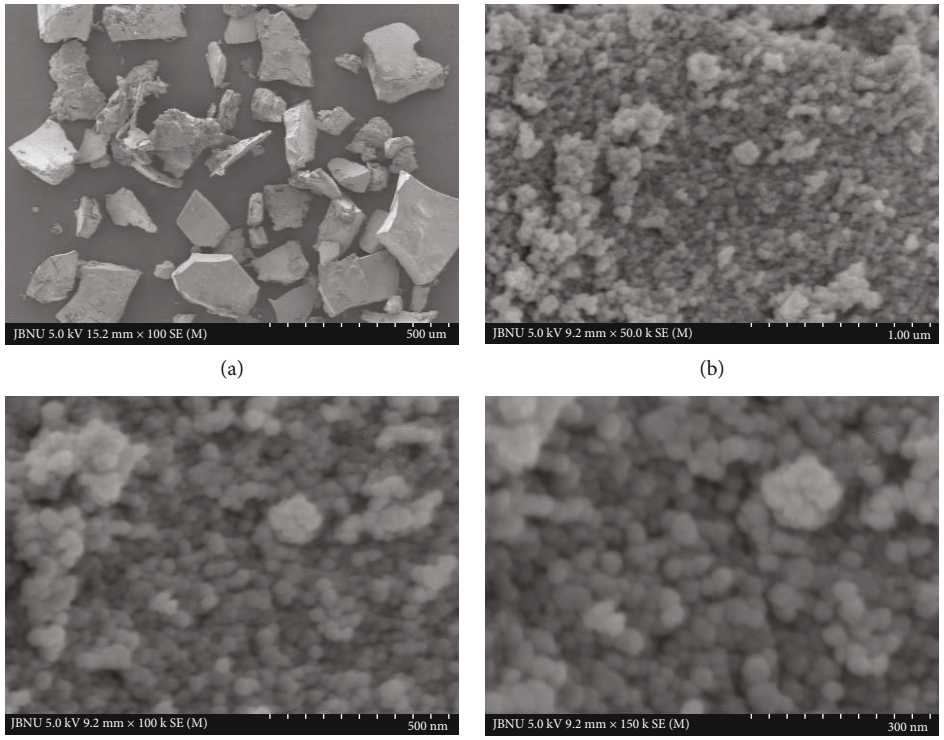


Figure 4: SEM images of the synthesized AgNPs.

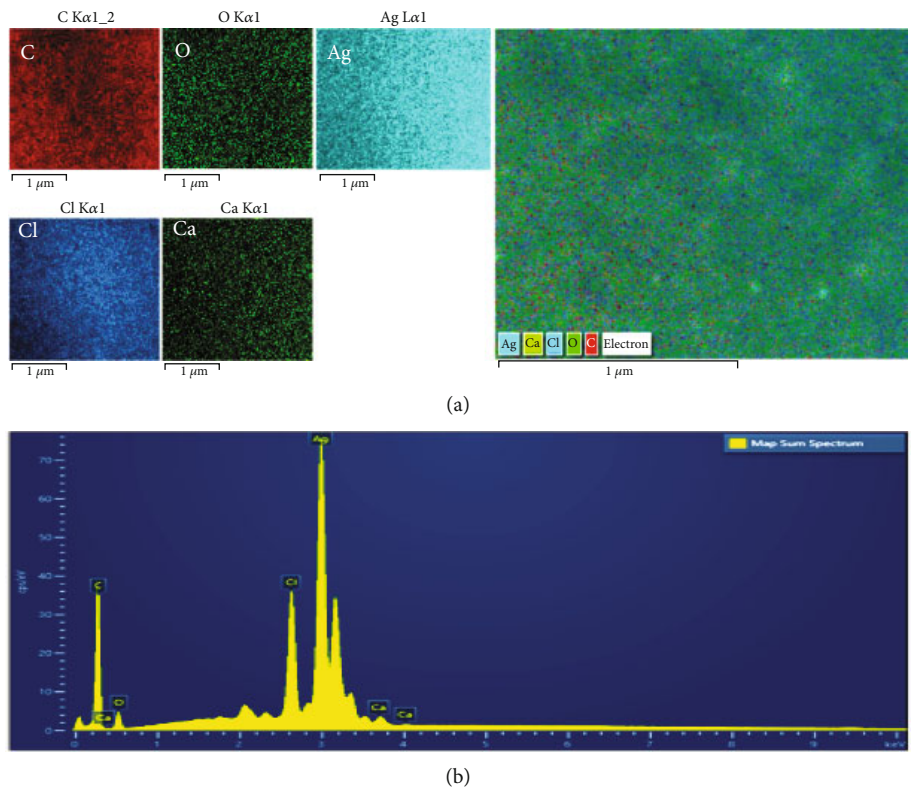


Figure 5: An energy-dispersive X-ray (EDX) spectrum of AgNPs with elemental mapping. (a) Total elemental mapping and color mapping for individual elements existing in synthesized AgNPs. (b) EDX spectrum of synthesized AgNPs.

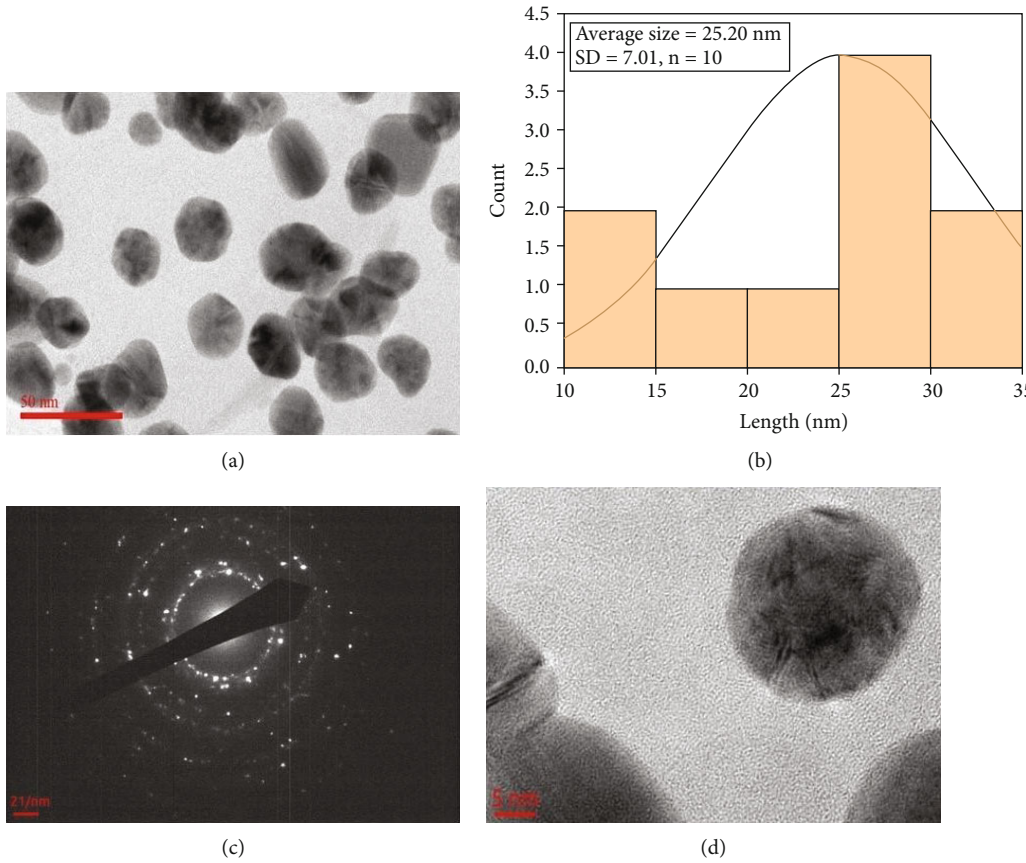


Figure 6: TEM images of the synthesized AgNPs. (a) Synthesized nanoparticles. (b) Mean size of the particles in the histogram. (c) SAED of synthesized AgNPs. (d) A single nanoparticle.

Table 2: Results of antioxidant activities of RERE and AgNPs.

Samples	IC_{50} (μg/mL)
R. ellipticus (aqueous extract)	15.86 ± 4.14
R. ellipticus (AgNPs)	13.83 ± 0.33
*Ascorbic acid	6.40 ± 0.29

Note: values are mean ± SD ($n = 3$); *ascorbic acid is a positive control.

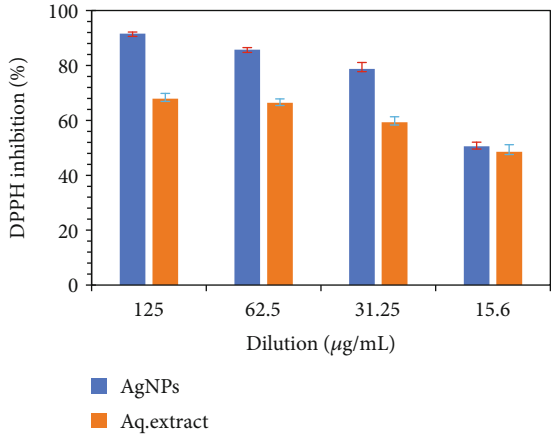


Figure 7: DPPH radical scavenging activity of RERE and AgNPs.

the Gram-positive and Gram-negative bacteria were evaluated for antibacterial susceptibility and the results are shown in Figure 8. Our results obtained from the agar well diffusion method had shown that the AgNPs displayed greater activity against all the tested bacteria. Table 3 shows that the ZOI values of RERE and AgNPs against *E. coli* increased from 10 mm to 13 mm, *S. aureus* increased from 9 mm to 12 mm, *E. faecalis* increased from 10 mm to12 mm, and *K. pneumoniae* increased from 11 mm to 14 mm. The maximum activity was exhibited against *K. pneumoniae*.

The AgNPs synthesized from *Areca catechu* showed dose-dependent zones of inhibition against antibiotic-resistant bacteria on the agar well diffusion method. The values of MIC and MBC of AgNPs revealed the substantial action on *Enterococcus faecalis* and Vancomycin-resistant *E. faecalis* (MIC = 11.25 μg/mL and MBC = 22.5 μg/mL), *Pseudomonas aeruginosa* and multidrug-resistant *P. aeruginosa* (MIC = 5.6 μg/mL and MBC = 22.5 μg/mL), and *Acinetobacter baumannii* and multidrug-resistant *A. baumannii* (MIC = 5.6 μg/mL, MBC = 22.5 μg/mL, and 11.25 μg/mL), respectively [50]. Rashid et al. [51] reported the increased antibacterial activity of AgNPs synthesized from the water extracts of the roots of *Bergenia ciliata*, *Bergenia stracheyi*, *Rumex dentatus*, and *Rumex hastatus* from Pakistani origin against six pathogenic bacteria including *E. coli*, *S. aureus*, *S. haemolyticus*, *Bacillus cereus*, *Salmonella typhi*, and

Table 3: Zones of inhibition (ZOI) of the tested bacteria against RERE and AgNPs.

Samples	Microorganisms			
	Escherichia coli	*Staphylococcus aureus*	*Enterococcus* faecalis	*Klebsiella pneumoniae*
RERE	10 mm	9 mm	10 mm	11 mm
AgNPs	13 mm	12 mm	12 mm	14 mm
PC	16 mm	16 mm	16 mm	15 mm

Note: PC = positive control (neomycin).

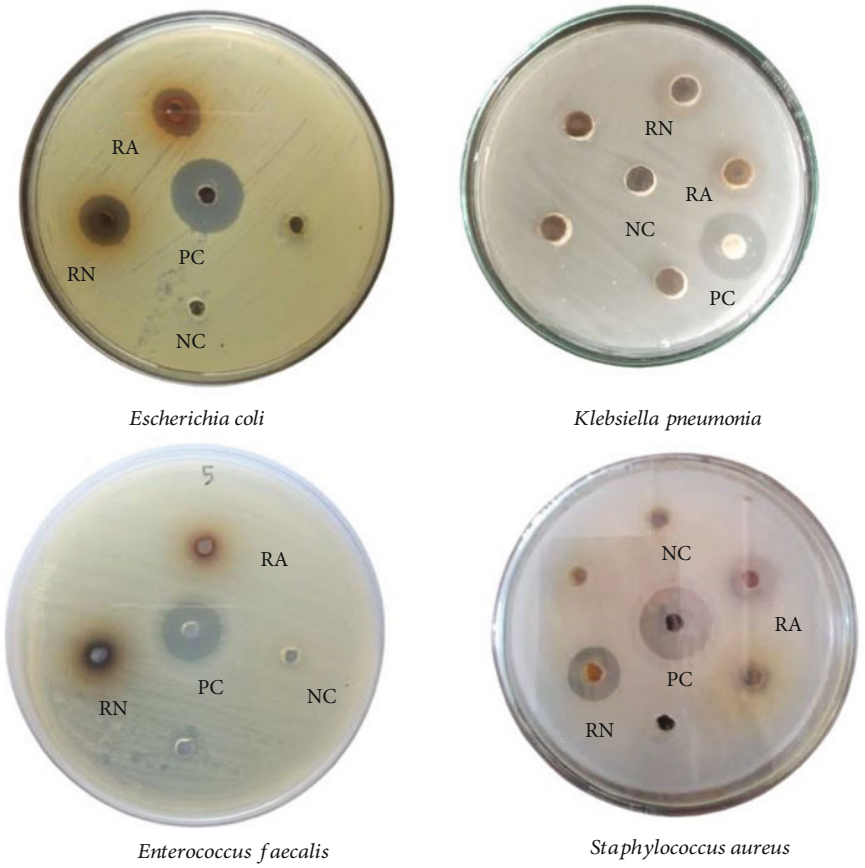


Figure 8: Antibacterial activity of RERE and synthesized AgNPs. Note: RA = RERE; RN = AgNPs; PC = positive control; NC = negative control.

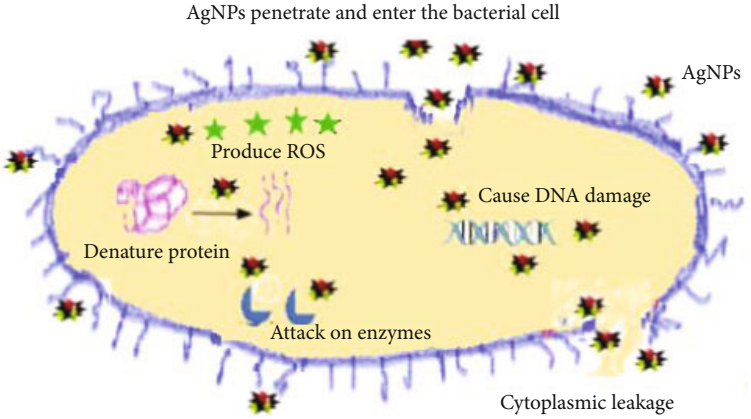


Figure 9: Schematic diagram of antibacterial activity of AgNPs.

Pseudomonas aeruginosa. In the agar well diffusion method, the AgNPs showed the inhibition zones ranging 7-15 mm, 10-16 mm, 8-16 mm, and 7-18 mm, respectively. The aqueous extracts of the plants were found inactive even at the doses of 1200 μg/well against all the bacteria used in the study compared to the positive control ($p < 0.05$). The crystalline AgNPs having an average size of 20 nm were synthesized by using the extracts of *Cestrum nocturnum* from India. They were reported to exhibit strong antibacterial activity against *Citrobacter*, *S. typhi*, and *E. coli* (MIC = 16 μg/mL); *Vibrio cholerae* and *Proteus vulgaris* (MIC = 8 μg/mL); and *E. faecalis* (MIC = 4 μg/mL) by the broth microdilution method. The plant extract was inactive towards all the bacteria in the disc diffusion method [52]. The aqueous extract of *Zataria multiflora* from Iran was used for the fabrication of AgNPs. The nanoparticles were monodispersed with an average size of 25.5 nm. They exhibited an elevated antibacterial activity in comparison to the commercial AgNPs against *S. aureus* with the minimum inhibitory concentrations of 4 and 8 μg/mL [53]. In a separate study, the AgNPs synthesized from the aqueous rhizome extracts of *Bergenia ciliata* of Pakistani origin were reported slightly higher antibacterial activities. The zones of inhibition were measured by the disc diffusion method. The AgNPs were inactive against *Micrococcus luteus* (ATCC 10240) but showed enhanced activities against *Bordetella bronchiseptica* (ATCC 4617), *S. aureus* (ATCC 6538), and *Enterobacter aerogenes* (ATCC 13048) which supports our results [46]. In this study, we found that our AgNPs showed greater activity against the Gram-negative (*E. coli* and *K. pneumoniae*) than Gram-positive (*E. faecalis* and *S. aureus*) bacteria. Urnukhsaikhan et al. [54] reported contradictory results in which the AgNPs synthesized from the aqueous extracts of *Carduus crispus* collected from Mongolia exhibited higher potency against Gram-positive bacteria *Micrococcus luteus* (ZOI = 7 ± 0.4 mm to 7.7 ± 0.5 mm) in comparison to the Gram-negative *E. coli* (ZOI = 5.5 ± 0.2 mm to 6.5 ± 0.3 mm). They had concluded that the antibacterial activity of different plant-based AgNPs does not depend on the thickness and texture of the bacterial cell wall only.

The antimicrobial potency of AgNPs depends upon various factors like shape, size, morphology, colloidal state, and the nature of bacteria. The AgNPs which have smaller sizes, irregular shapes, and larger surface areas show relatively higher antibacterial activities. The relatively thin lipid layer of Gram-negative bacteria is easily penetrated by the smaller AgNPs leading to the damage of the bacterial cells [55].

The accurate antimicrobial mechanism of AgNPs has been studied extensively but is not hitherto authenticated. Many propositions explain the antibacterial activity of AgNPs which can be depicted in Figure 9. The silver nanoparticles destroy the bacteria via the generation of reactive oxygen species (ROS), the release of Ag^+ ions from AgNPs that denaturize proteins bonding sulfhydryl group, and the gripping of AgNPs on bacteria resulting in cell damage [54]. Similarly, it is hypothesized that the AgNPs get stuck to the bacteria, interact with the cell wall, and kill them by interrupting the membrane permeability. It is also explained that the AgNPs break down the cells or disturb cell functions by interacting with amino acids and enzymes and generating reactive oxygen species. Silver nanoparticles interact with the soft bases like sulphur and phosphorus present in the nucleus, damage DNA, and ultimately cause cell death[56, 57].

4. Conclusion

This study established a simple, easier, and eco-friendly technique of synthesizing AgNPs from the aqueous extracts of root barks of a commonly used medicinal plant, *R. ellipticus* Sm. The observation of shifting of the peaks in the FTIR spectra indicated the potential role of different functional groups of plant secondary metabolites as capping and stabilizing agents. The fcc crystallinity and spherical morphology of the particles were established by the XRD and FESEM measurements. The relative abundance of silver, oxygen, carbon, calcium, and chlorine was revealed by the EDX analysis. The TEM image analysis shows the size of the nanoparticles ranging from 13.85 to 34.30 nm with an average size of 25.20 ± 7.01 nm. The synthesized AgNPs were found to exhibit higher antibacterial and antioxidant activity as compared to the aqueous extract. Further works on the possible effects of the size, morphology, and phytochemicals on physicochemical parameters are warranted to enable greater optimization of the biological activities of the AgNPs. Hence, the biosynthetic technique might be an alternative to chemical and physical methods indicating the possibility of the plant for the development of different products for biological and medical applications.

Data Availability

The data obtained in this study are available from the corresponding author upon request.

Conflicts of Interest

All the authors declare no conflicts of interest.

Acknowledgments

Prithvi Narayan Campus, Pokhara provided Ph.D. study leave to the first author. The Jeonbuk National University, Jeonju, South Korea, is acknowledged for the XRD, FESEM, EDX, and TEM analysis of the synthesized nanoparticles.

References

[1] M. Kandiah and K. N. Chandrasekaran, "Green synthesis of silver nanoparticles using Catharanthus roseus flower extracts and the determination of their antioxidant, antimicrobial, and photocatalytic activity," *Journal of Nanotechnology*, vol. 2021, Article ID 5512786, 18 pages, 2021.

[2] S. Gurunathan, K. Kalishwaralal, R. Vaidyanathan et al., "Biosynthesis, purification and characterization of silver nanoparticles using *Escherichia coli*," *Colloids and Surfaces B: Biointerfaces*, vol. 74, no. 1, pp. 328–335, 2009.

[3] S. Pirtarighat, M. Ghannadnia, and S. Baghshahi, "Green synthesis of silver nanoparticles using the plant extract of Salvia spinosa grown in vitro and their antibacterial activity assessment," *Journal of Nanostructure in Chemistry*, vol. 9, no. 1, pp. 1–9, 2019.

[4] S. H. Jeong, S. Y. Yeo, and S. C. Yi, "The effect of filler particle size on the antibacterial properties of compounded polymer/silver fibers," *Journal of Materials Science*, vol. 40, no. 20, pp. 5407–5411, 2005.

[5] S. Ahmed, M. Ahmad, B. L. Swami, and S. Ikram, "A review on plants extract mediated synthesis of silver nanoparticles for antimicrobial applications: a green expertise," *Journal of Advanced Research*, vol. 7, no. 1, pp. 17–28, 2016.

[6] S. Salari, S. E. Bahabadi, A. Samzadeh-Kermani, and F. Yosefzaei, "In-vitro evaluation of antioxidant and antibacterial potential of green synthesized silver nanoparticles using Prosopis farcta fruit extract," *Iranian Journal of Pharmaceutical Research*, vol. 18, no. 1, pp. 430–445, 2018.

[7] E. Abbasi, M. Milani, S. F. Aval et al., "Silver nanoparticles: synthesis methods, bio-applications and properties," *Critical Reviews in Microbiology*, vol. 42, no. 2, pp. 173–180, 2016.

[8] Z. Bedlovičová, I. Strapáč, M. Baláž, and A. Salayová, "A brief overview on antioxidant activity determination of silver nanoparticles," *Molecules*, vol. 25, no. 14, pp. 1–24, 2020.

[9] S. Rajeshkumar, C. Malarkodi, K. Paulkumar, M. Vanaja, G. Gnanajobitha, and G. Annadurai, "Algae mediated green fabrication of silver nanoparticles and examination of its antifungal activity against clinical pathogens," *International Journal of Metals*, vol. 2014, Article ID 692643, 8 pages, 2014.

[10] H. Barabadi, A. Mohammadzadeh, H. Vahidi et al., "Penicillium chrysogenum-derived silver nanoparticles: exploration of their antibacterial and biofilm inhibitory activity against the standard and pathogenic Acinetobacter baumannii compared to tetracycline," *Journal of Cluster Science*, vol. 2021, pp. 1–14, 2021.

[11] G. Rahimi, F. Alizadeh, and A. Khodavandi, "Mycosynthesis of silver nanoparticles from *Candida albicans* and its antibacterial activity against *Escherichia coli* and *Staphylococcus aureus*," *Tropical Journal of Pharmaceutical Research*, vol. 15, no. 2, pp. 371–375, 2016.

[12] B. Gowramma, U. Keerthi, M. Rafi, and D. Muralidhara Rao, "Biogenic silver nanoparticles production and characterization from native stain of Corynebacterium species and its antimicrobial activity," *Biotech*, vol. 5, no. 2, pp. 195–201, 2015.

[13] M. I. Masum, M. M. Siddiqa, K. A. Ali et al., "Biogenic synthesis of silver nanoparticles using *Phyllanthus emblica* fruit extract and its inhibitory action against the pathogen *Acidovorax oryzae* strain RS-2 of rice bacterial brown stripe," *Frontiers in Microbiology*, vol. 10, pp. 1–18, 2019.

[14] A. C. Paiva-Santos, A. M. Herdade, C. Guerra et al., "Plant-mediated green synthesis of metal-based nanoparticles for dermopharmaceutical and cosmetic applications," *International Journal of Pharmaceutics*, vol. 597, pp. 120311–120328, 2021.

[15] A. Hussain, A. Mehmood, G. Murtaza et al., "Environmentally benevolent synthesis and characterization of silver nanoparticles using Olea ferruginea Royle for antibacterial and antioxidant activities," *Green Processing and Synthesis*, vol. 9, no. 1, pp. 451–461, 2020.

[16] H. M. M. Ibrahim, "Green synthesis and characterization of silver nanoparticles using banana peel extract and their antimicrobial activity against representative microorganisms," *Journal of Radiation Research and Applied Sciences*, vol. 8, no. 3, pp. 265–275, 2015.

[17] F. Sharifi, F. Sharififar, S. Soltanian, M. Doostmohammadi, and N. Mohamadi, "Synthesis of silver nanoparticles using salvia officinalis extract: structural characterization, cytotoxicity, antileishmanial and antimicrobial activity," *Nanomedicine Research Journal*, vol. 5, no. 4, pp. 339–346, 2020.

[18] R. S. Priya, D. Geetha, and P. S. Ramesh, "Antioxidant activity of chemically synthesized AgNPs and biosynthesized *Pongamia pinnata* leaf extract mediated AgNPs - a comparative study," *Ecotoxicology and Environmental Safety*, vol. 134, Part 2, pp. 308–318, 2016.

[19] M. S. Abdel-Aziz, M. S. Shaheen, A. A. El-Nekeety, and M. A. Abdel-Wahhab, "Antioxidant and antibacterial activity of silver nanoparticles biosynthesized using *Chenopodium murale* leaf extract," *Journal of Saudi Chemical Society*, vol. 18, no. 4, pp. 356–363, 2014.

[20] M. S. Jabir, A. A. Hussien, G. M. Sulaiman et al., "Green synthesis of silver nanoparticles fromEriobotrya japonicaextract: a promising approach against cancer cells proliferation, inflammation, allergic disorders and phagocytosis induction," *Artificial Cells, Nanomedicine and Biotechnology*, vol. 49, no. 1, pp. 48–60, 2021.

[21] D. Garibo, H. A. Borbón-Nuñez, J. N. D. de León et al., "Green synthesis of silver nanoparticles using *Lysiloma acapulcensis* exhibit high-antimicrobial activity," *Scientific Reports*, vol. 10, no. 1, p. 12805, 2020.

[22] A. Badhani, S. Rawat, I. D. Bhatt, and R. S. Rawal, "Variation in chemical constituents and antioxidant activity in yellow Himalayan (*Rubus ellipticus* Smith) and hill raspberry (Rubus Niveus Thunb.)," *Journal of Food Biochemistry*, vol. 39, no. 6, pp. 663–672, 2015.

[23] B. P. George, T. Parimelazhagan, Y. T. Kumar, and T. Sajeesh, "Antitumor and wound healing properties of *Rubus ellipticus* Smith.," *Journal of Acupuncture and Meridian Studies*, vol. 8, no. 3, pp. 134–141, 2015.

[24] L. N. Khanal, K. R. Sharma, Y. R. Pokharel, and S. K. Kalauni, "Assessment of phytochemical, antioxidant and antimicrobial activities of some medicinal plants from Kaski district of Nepal," *American Journal of Plant Sciences*, vol. 11, no. 9, pp. 1383–1397, 2020.

[25] B. Adebayo-Tayo, A. Salaam, and A. Ajibade, "Green synthesis of silver nanoparticle using *Oscillatoria* sp. extract, its antibacterial, antibiofilm potential and cytotoxicity activity," *Heliyon*, vol. 5, no. 10, pp. e02502–e02508, 2019.

[26] A. Rautela, J. Rani, and M. Debnath (Das), "Green synthesis of silver nanoparticles from Tectona grandis seeds extract: characterization and mechanism of antimicrobial action on different microorganisms," *Journal of Analytical Science and Technology*, vol. 10, no. 1, pp. 2–10, 2019.

[27] M. E. Taghavizadeh Yazdi, A. Hamidi, M. S. Amiri et al., "Eco-friendly and plant-based synthesis of silver nanoparticles usingAllium giganteumand investigation of its bactericidal, cytotoxicity, and photocatalytic effects," *Materials Technology*, vol. 34, no. 8, pp. 490–497, 2019.

[28] W. Brand-Williams, M. E. Cuvelier, and C. Berset, "Use of a free radical method to evaluate antioxidant activity," *LWT-Food science and Technology*, vol. 28, no. 1, pp. 25–30, 1995.

[29] S. C. Liu, J. T. Lin, C. K. Wang, H. Y. Chen, and D. J. Yang, "Antioxidant properties of various solvent extracts from lychee (*Litchi chinenesis* Sonn.) flowers," *Food Chemistry*, vol. 114, no. 2, pp. 577–581, 2009.

[30] P. R. Murray, E. J. Baron, M. L. Landry, J. H. Jorgensen, and M. A. Pfallier, *Manual of Clinical Microbiology (9th ed., Vol. 1)*, American Society for Microbiology, 2007.

[31] S. Ahmed, A. Saifullah, M. Swami, B. L. Swami, and S. Ikram, "Green synthesis of silver nanoparticles usingAzadirachta indicaaqueous leaf extract," *Journal of Radiation Research and Applied Sciences*, vol. 9, no. 1, pp. 1–7, 2016.

[32] M. Bhagat, S. Rajput, S. Arya, S. Khan, and P. Lehana, "Biological and electrical properties of biosynthesized silver nanoparticles," *Bulletin of Materials Science*, vol. 38, no. 5, pp. 1253–1258, 2015.

[33] P. K. Tyagi, S. Tyagi, D. Gola et al., "Ascorbic acid and polyphenols mediated green synthesis of silver nanoparticles from *Tagetes erecta* L. aqueous leaf extract and studied their antioxidant properties," *Journal of Nanomaterials*, vol. 2021, Article ID 6515419, 9 pages, 2021.

[34] S. M. Ali, N. M. H. Yousef, and N. A. Nafady, "Application of biosynthesized silver nanoparticles for the control of land snail eobania vermiculata and some plant pathogenic fungi," *Journal of Nanomaterials*, vol. 2015, Article ID 218904, 10 pages, 2015.

[35] P. K. Kaman and P. Dutta, "Synthesis, characterization and antifungal activity of biosynthesized silver nanoparticle," *Indian Phytopathology*, vol. 72, no. 1, pp. 79–88, 2019.

[36] J. Venkatesan, S. K. Kim, and M. S. Shim, "Antimicrobial, antioxidant, and anticancer activities of biosynthesized silver nanoparticles using marine algae Ecklonia cava," *Nanomaterials*, vol. 6, no. 12, pp. 1–18, 2016.

[37] A. Baran, M. F. Baran, C. Keskin et al., "Ecofriendly/rapid synthesis of silver nanoparticles using extract of waste parts of artichoke (Cynara scolymus L.) and evaluation of their cytotoxic and antibacterial activities," *Journal of Nanomaterials*, vol. 2021, Article ID 2270472, 10 pages, 2021.

[38] A. Afreen, R. Ahmed, S. Mehboob et al., "Phytochemical-assisted biosynthesis of silver nanoparticles from Ajuga bracteosa for biomedical applications," *Materials Research Express*, vol. 7, no. 7, pp. 1–14, 2020.

[39] P. R. M. Hemlata, A. P. Singh, and K. K. Tejavath, "Biosynthesis of silver nanoparticles usingCucumis prophetarum aqueous leaf extract and their antibacterial and antiproliferative activity against cancer cell lines," *ACS Omega*, vol. 5, no. 10, pp. 5520–5528, 2020.

[40] B. K. Mehta, M. Chhajlani, and B. D. Shrivastava, "Green synthesis of silver nanoparticles and their characterization by XRD," *Journal of Physics: Conference Series*, vol. 836, no. 1, p. 012050, 2017.

[41] A. Fouda, S. E. D. Hassan, A. M. Abdo, and M. S. El-Gamal, "Antimicrobial, antioxidant and larvicidal activities of spherical silver nanoparticles synthesized by endophytic Streptomyces spp," *Biological Trace Element Research*, vol. 195, no. 2, pp. 707–724, 2020.

[42] V. Ravichandran, S. Vasanthi, S. Shalini, S. A. A. Shah, and R. Harish, "Green synthesis of silver nanoparticles using *Atrocarpus altilis* leaf extract and the study of their antimicrobial and antioxidant activity," *Materials Letters*, vol. 180, pp. 264–267, 2016.

[43] T. Y. Suman, S. R. Radhika Rajasree, A. Kanchana, and S. B. Elizabeth, "Biosynthesis, characterization and cytotoxic effect of plant mediated silver nanoparticles using *Morinda citrifolia* root extract," *Colloids and Surfaces B: Biointerfaces*, vol. 106, pp. 74–78, 2013.

[44] E. E. Elemike, O. E. Fayemi, A. C. Ekennia, D. C. Onwudiwe, and E. E. Ebenso, "Silver nanoparticles mediated by costus afer leaf extract: synthesis, antibacterial, antioxidant and electrochemical properties," *Molecules*, vol. 22, no. 5, pp. 1–20, 2017.

[45] S. Bhakya, S. Muthukrishnan, M. Sukumaran et al., "Antimicrobial, antioxidant and anticancer activity of biogenic silver nanoparticles-an experimental report," *RSC Advances*, vol. 6, no. 84, pp. 81436–81446, 2016.

[46] A.-R. Phull, Q. Abbas, A. Ali et al., "Antioxidant, cytotoxic and antimicrobial activities of green synthesized silver nanoparticles from crude extract of *Bergenia ciliata*," *Future Journal of Pharmaceutical Sciences*, vol. 2, no. 1, pp. 31–36, 2016.

[47] V. Kumar, S. Singh, B. Srivastava, R. Bhadouria, and R. Singh, "Green synthesis of silver nanoparticles using leaf extract of *Holoptelea integrifolia* and preliminary investigation of its antioxidant, anti- inflammatory, antidiabetic and antibacterial activities," *Journal of Environmental Chemical Engineering*, vol. 7, no. 3, pp. 103094–103097, 2019.

[48] M. S. Akhtar, M. K. Swamy, A. Umar, and A. A. al Sahli, "Biosynthesis and characterization of silver nanoparticles from methanol leaf extract of Cassia didymobotyra and assessment of their antioxidant and antibacterial activities," *Journal of Nanoscience and Nanotechnology*, vol. 15, no. 12, pp. 9818–9823, 2015.

[49] M. A. Raza, Z. Kanwal, A. Rauf, A. N. Sabri, S. Riaz, and S. Naseem, "Size- and shape-dependent antibacterial studies of silver nanoparticles synthesized by wet chemical routes," *Nanomaterials*, vol. 6, no. 4, p. 74, 2016.

[50] J. S. Choi, H. C. Jung, Y. J. Baek et al., "Antibacterial activity of green-synthesized silver nanoparticles using *Areca catechu* extract against antibiotic-resistant bacteria," *Nanomaterials*, vol. 11, no. 1, pp. 1–16, 2021.

[51] S. Rashid, M. Azeem, S. A. Khan, M. M. Shah, and R. Ahmad, "Characterization and synergistic antibacterial potential of green synthesized silver nanoparticles using aqueous root extracts of important medicinal plants of Pakistan," *Colloids and Surfaces B: Biointerfaces*, vol. 179, pp. 317–325, 2019.

[52] A. K. Keshari, R. Srivastava, P. Singh, V. B. Yadav, and G. Nath, "Antioxidant and antibacterial activity of silver nanoparticles synthesized by *Cestrum nocturnum*," *Journal of Ayurveda and Integrative Medicine*, vol. 11, no. 1, pp. 37–44, 2020.

[53] H. Barabadi, F. Mojab, H. Vahidi et al., "Green synthesis, characterization, antibacterial and biofilm inhibitory activity of silver nanoparticles compared to commercial silver nanoparticles," *Inorganic Chemistry Communications*, vol. 129, p. 108647, 2021.

[54] E. Urnukhsaikhan, B.-E. Bold, A. Gunbileg, N. Sukhbaatar, and T. Mishig-Ochir, "Antibacterial activity and characteristics of silver nanoparticles biosynthesized from *Carduus crispus*," *Scientific Reports*, vol. 11, no. 1, article 21047, 2021.

[55] T. C. Dakal, A. Kumar, R. S. Majumdar, and V. Yadav, "Mechanistic basis of antimicrobial actions of silver nanoparticles," *Frontiers in Microbiology*, vol. 7, no. 1831, pp. 1–17, 2016.

[56] R. H. Ahmed and D. E. Mustafa, "Green synthesis of silver nanoparticles mediated by traditionally used medicinal plants in Sudan," *International Nano Letters*, vol. 10, no. 1, pp. 1–14, 2020.

[57] H. Veisi, S. Hemmati, H. Shirvani, and H. Veisi, "Green synthesis and characterization of monodispersed silver nanoparticles obtained using oak fruit bark extract and their antibacterial activity," *Applied Organometallic Chemistry*, vol. 30, no. 6, pp. 387–391, 2016.